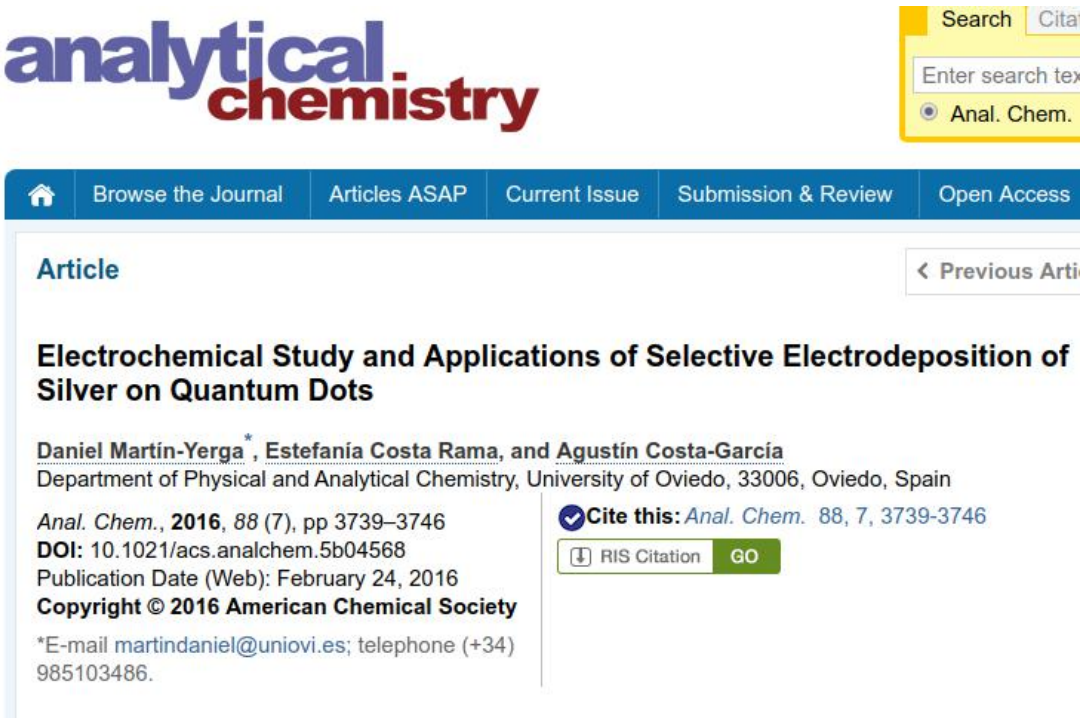

GRAPHICAL TABLE OF CONTENTS

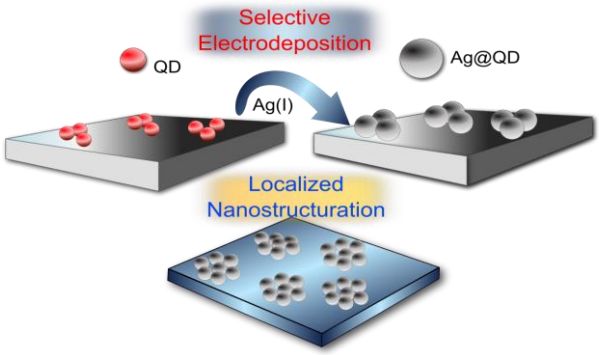

Silver nanoparticles can be selectively electrodeposited on quantum dots. It could be used for the generation of localized silver nanostructured surfaces and sensing applications.

Electrochemical study and applications of the selective electrodeposition of silver on quantum dots

Daniel Martín-Yerga*, Estefanía Costa Rama and Agustín Costa-García

Department of Physical and Analytical Chemistry, University of Oviedo, 33006, Oviedo (Spain)

* Corresponding author: Daniel Martín-Yerga

Department of Physical and Analytical Chemistry

University of Oviedo Oviedo

Julián Clavería 8, 33006, Oviedo (Spain)

E-mail: martindaniel@uniovi.es

Telephone: (+34) 985103486

ABSTRACT

In this work, the selective electrodeposition of silver on quantum dots is described. The particular characteristics of the nanostructured silver thus obtained are studied by electrochemical and microscopic techniques. On one hand, the quantum dots were found to catalyse the silver electrodeposition, and on the other hand, a strong adsorption between the electrodeposited silver and quantum dots was observed, indicated by two silver stripping processes. Nucleation of silver nanoparticles followed different mechanisms depending on the surface (carbon or quantum dots). Voltammetric and confocal microscopy studies showed the great influence of the electrodeposition time in the surface coating and high-resolution transmission electron microscopy (HRTEM) imaging confirmed the initial formation of Janus-like Ag@QDs nanoparticles in this process. Using moderate electrodeposition conditions such as 50 μM of silver, -0.1 V and 60 s, the silver was only deposited on quantum dots, allowing the generation of localized nanostructured electrode surfaces. This methodology can also be employed for sensing applications, showing a promising ultrasensitive electrochemical method for quantum dots detection.

KEYWORDS: electrodeposition, nanostructuration, silver nanoparticles, quantum dots, screen-printed electrodes.

INTRODUCTION

Nanotechnology has emerged as one of the brightest scientific trends of the recent years, and, aside from the inherent scientific interest, it is currently having a vast number of applications in the real world. The generation of functional nanostructured surfaces is a subject of study in many fields and the development of new methodologies for fabricating these surfaces is a constant concern. Electrochemistry has emerged as one of the most interesting techniques to generate localized nanostructures by electrodeposition. The possibility to select the experimental parameters allows a high control of the size and characteristics of the generated nanostructures. For instance, scanning probe techniques such as scanning electrochemical microscopy (SECM) have been used for localized generation of nanostructured surfaces[1–4]. Although these techniques allow a very specific control of the deposition sites due to the utilization of micro or nanoelectrodes and a piezoelectric control system, they are quite complex and time-consuming if a large surface needs to be coated with localized nanostructures. This fact makes these techniques not acceptable for generating nanostructured surfaces on a large scale or for macroscopic surfaces. An alternative is the use of bipolar electrochemistry[5] for localized deposition in conducting objects. Bipolar electrochemistry has been used to generate Janus-like objects such as carbon tubes or glassy carbon spheres modified with metals at only one end[6,7]. Although useful for objects like microparticles, bipolar electrochemistry does not seem suitable for localized nanostructuration of macroscopic surfaces. Other works have been published in which metal nanoparticles are electrodeposited on carbon nanomaterials such as carbon nanotubes[8,9] or graphene[10,11]. Interestingly, the metal nanoparticles seem to have a preference for electrodeposition in specific areas of the graphene or carbon nanotubes. However, in these works, the working electrode consists of the nanomaterial, which is grown on a non-conductive substrate. It does not seem clear that the metal nanoparticles could be selectively electrodeposited on the nanomaterials if the substrate was conductive. Therefore, it seems that a simple, fast and inexpensive methodology, which could be used to coat a macroscopic surface with metal nanostructures only in selected areas remains to be published.

On the other hand, silver electrodeposition has been extensively studied at different surfaces and experimental conditions[12,13]. It has been found that silver can be electrodeposited catalytically on gold nanoparticles[14,15]. However, the electrodeposition of silver on surfaces modified with quantum dots (QDs) has not been reported. QDs are semiconductor crystalline nanoparticles with very interesting photoluminescent properties and are widely employed in solar cells or bioanalysis[16]. QDs typically have a roughly spherical shape and a diameter between 2-8 nm, although the functional coating could increase this size. At these small sizes, nanoparticles behave differently to the macroscopic materials due to effects of the quantum confinement. For instance, the energy structure of these nanoparticles is converted to discrete levels and surface properties are extremely important due to its high surface-to-volume ratio. Interestingly, these crystals may have defects in their structure that can act as trap sites for both electrons and holes, thereby constituting oxidizing and reducing centres, respectively[17,18]. QDs have been widely used as detection labels in electrochemical biosensing[19,20]. Metallic components of the QDs can be easily measured electrochemically after an acid attack to release the metals to the solution[21]. Generally, the bioassay is performed outside the detection platform and after releasing the metals, the solution is transferred to the electrochemical cell[22,23]. In our research group, we have developed a methodology that allows to carry out the bioassay and the electrochemical detection using screen-printed electrodes and avoiding the solution transfer[24–26]. However, an acid attack is also necessary to achieve the detection of low QDs concentrations. This fact, although improves the sensitivity and the procedure complexity, is not yet ideal. Therefore, the development of a methodology for the electrochemical detection of low QDs concentrations without an acid attack, could significantly improve the QDs-based electrochemical biosensors.

In this work, we describe the selective electrodeposition of silver on a surface modified with quantum dots. The electrochemical processes involving the selective electrodeposition are thoroughly evaluated. This strategy allows to electrodeposit silver nanoparticles only at zones of a surface where quantum dots are

found and localized nanostructured surfaces can be fabricated. A very selective stripping process is also found for the electrodeposited silver, which it is useful for the ultrasensitive determination of quantum dots, and sensing applications.

EXPERIMENTAL

Apparatus and electrodes

Voltammetric measurements were performed with an Autolab PGSTAT 12 (Eco Chemie, The Netherlands) potentiostat/galvanostat interfaced to an AMD K6 266 MHz computer system and controlled by Autolab GPES 4.9. All measurements were carried out at room temperature.

Screen-printed carbon electrodes (SPCEs) were purchased from DropSens (Spain). These electrodes incorporate a conventional three-electrode configuration, printed on ceramic substrates (3.4 x 1.0 cm). Both working (disk-shaped 4 mm diameter) and counter electrodes are made of carbon inks, whereas pseudoreference electrode and electric contacts are made of silver. The SPEs were connected to the potentiostat through a specific connector (DropSens, ref. DSC). A custom-made Ag/AgCl reference electrode (in saturated KCl) was employed for a better control of the applied potential. The fabrication of this electrode is briefly described in the Supporting Information (S.I.). The external reference electrode was placed close to the working electrode with the aim to minimize the cell uncompensated resistance (Ru).

A JEOL 6610LV scanning electron microscope was used to characterize the working electrodes. ImageJ software was used for the estimation of the nanoparticles size in the SEM images. A JEOL JEM-2100 transmission electron microscope was used to study the initial formation of the Ag@QDs nanoparticle hybrid. Carbon-coated copper TEM grids were used in order to carry out the electrodepostion as reported elsewhere[27] using an electrochemical cell described in the S.I. A Leica SP8X Confocal microscope was used in order to visualize the fluorescence of the QDs-modified electrodes. A laser of 405 nm from the microscope was employed for the QDs excitation and the fluorescence was detected in a range between

635 and 675 nm. For the confocal microscopy, the QDs-modified electrodes were previously photo-activated under a 365 nm UV lamp (6W, Vilbert Lourmat) for 15 minutes.

Reagents and solutions

Ammonia solution (30%) was purchased from Merck. Tris(hydroxymethyl)aminomethane (Tris), silver, copper, zinc, nickel and cobalt nitrates were purchased from Sigma-Aldrich. Qdot® 655 Biotin Conjugate (QDs) was purchased from Life Technologies (Spain). Ultrapure water obtained with a Millipore Direct Q5™ purification system from Millipore Ibérica S.A. (Madrid, Spain) was used throughout this work. All other reagents were of analytical grade. Working solutions of QDs were prepared in 0.1 M pH 7.4 Tris-HCl buffer. QDs concentration is given as particle concentration throughout this work. A drop of 10 µL of a 10 nM QDs solution was employed for electrode modification unless stated otherwise.

Electrochemical detection of quantum dots

Briefly, the procedure for the electrochemical detection of quantum dots using the selective electrodeposition of silver was as follows: QDs were adsorbed on the electrode surface by placing a drop of 10 µL on the working electrode. The adsorption time was maximal at 30 min and the analytical signal did not increase even left overnight at 4 ºC. After washing with H_2O, a drop of 40 µL of 250 µM $AgNO_3$ in 1 M NH_3 was added to the screen-printed card, and a potential of -0.2 V for 60 s was applied to carry out the electrodeposition. A potential of +0.8 V for 15 s was applied before the electrodeposition in order to decrease the capacitive current and to obtain a better shaped stripping peak. The stripping of the deposited silver is performed by differential-pulse voltammetry between +0.2 and +0.7 V with the following parameters: 0.1 V for modulation amplitude, 0.01 V for step potential, 0.03 s for modulation time, 0.1 s for interval time, and 5 s for equilibration time.

RESULTS AND DISCUSSION

Electrochemical study of silver electrodeposition on quantum dots

As the electrodeposition of silver on quantum dots-modified electrodes had not been previously reported, a thorough electrochemical study of the silver electrodeposition on quantum dots was carried out. Firstly, the cyclic voltammetry (CV) of silver using bare screen-printed carbon electrodes and modified with quantum dots was performed. As shown in the Figure 1, the electrochemical behaviour of silver on quantum dots-modified electrodes is different than on bare carbon electrodes. The typical processes observed for the electrodeposition and stripping of silver are observed at -0.5 V and +0.05 V, respectively. However, new cathodic and anodic processes appeared on the voltammogram when quantum dots are presented on the electrode surface. This cathodic process appeared at a more positive potential (-0.1 V) than the normal deposition. This indicates that the reduction of silver is carried out applying less energy than for the bulk deposition. Quantum dots showed a catalytic effect on the electrodeposition of silver. In the same way, the new anodic process appeared at a more positive potential than the bulk stripping, indicating that a higher energy should be applied to achieve the stripping of silver from the quantum dots. This fact indicates a strong interaction between the electrodeposited silver and the quantum dots. These processes can be observed in LSV experiments considering only the cathodic and anodic waves, as shown in Figure S2 (see S.I).

Although the cationic exchange between metals inside the quantum dots structure and metals in solution has been reported[28], even at room temperature[29], this fact does not happen under the experimental conditions and timescale of this experiment. If the cation exchange occurred, ionic silver would be introduced in the nanoparticle structure and would be strongly combined with nanoparticle ligands (probably with sulphur, which it is in the nanoparticle shell). Therefore, the reduction of silver from the nanoparticle would be more difficult than the bulk silver and would occur at a more negative potential. The fact that the reduction of silver interacting with the quantum dots occurs at a more positive potential than the bulk reduction means

that ionic silver is not strongly interacting with the nanoparticles before the reduction. Bard et al. reported that QDs could be involved in multielectron transfer at a given potential due to trapping of electrons within the particle[30]. This fact strongly agree with the electrochemical response found for the electrodeposition of silver on quantum dots. Due to the potential sweep, the QDs may be accepting and trapping electrons in its structure, which are then transferred to the locally surrounding Ag(I) ions producing its reduction on the semiconductor nanoparticles. Lisdat et al. described that CdSe/ZnS QDs could produce the reduction of ferrocyanide in solution after the application of light pulses. It is not unreasonable to think that a similar process may occur in this case, where the QDs are excited by electron transfer from the electrode (or even by ambient light) and the excited electrons could be transferred to the silver. Ferrocyanide has a reduction potential relatively close to silver reduction, and, therefore, it could be a similar process. After the deposition of silver, a strong interaction between the nanoparticle surface and electrodeposited silver is found as indicated by the high stripping overpotential. This fact is probably due to the small size of quantum dots, where the surface processes are enhanced by the high surface-to-volume ratio. The following mechanism is proposed for silver reduction and oxidation processes involving QDs:

$$QD + 1\,e^- \rightarrow QD(e^-)$$

$$Ag(NH_3)_2^+ + QD(e^-) \rightarrow Ag(QD) + 2\,NH_3$$

$$Ag(QD) + 2\,NH_3 \rightarrow Ag(NH_3)_2^+ + 1\,e^-$$

In order to evaluate the rate-limiting step of the different electrochemical processes, linear sweep voltammograms at different scan rates were recorded. In the Figure S3, the effect of the scan rate in the anodic and cathodic processes is shown. The linear relationship between the peak current and the square root of the scan rate for the reduction processes indicates that the rate-limiting step of the electrodeposition is diffusion-controlled (mass transport of $[Ag(NH_3)_6]^+$ ions to the electrode surface), confirming that the cation exchange is not occurring. In order to study the stripping processes, the electrodeposition of silver was performed (-0.1 V for 60 s) before recording the voltammograms. The linear relationship between the

peak current and the scan rate indicates that the rate-limiting step for the stripping processes is adsorption-controlled. The great difference found between the peak potential of the bulk and QDs-involved silver stripping processes shows that a strong adsorption between the elemental silver and quantum dots occurs.

A high control of the deposition parameters (deposition potential and time, and the concentration of ionic silver) allows to obtain some experimental conditions in which only the selective deposition of silver onto the surface of quantum dots is produced instead of over the entire surface. A study of accumulation at different deposition times was performed. Electrodeposition was carried out using a solution of 50 µM of Ag(I) in 1 M NH_3 applying -0.1 V for different times. An electrode modified with 10 µL of 10 nM QDs was employed. In the Figure 2, the clear effect of the deposition time on the stripping processes is shown. At low deposition times, only the stripping process at +0.45 V appears, and the peak current increases with the deposition time. At 120 s, a small peak current appears at 0.05 V, indicating that quantum dots active sites are saturated. At higher deposition times, the peak current of the process at 0.05 V experiences a significant increment due to that the silver deposited after the saturation of QDs does not show any difference to the normal silver deposition, i. e., specific interaction with the QDs is not observed after saturation. The peak current at +0.45 V no longer increases with time, which also indicates the saturation. The effect of the electrodepostion time was also evaluated by confocal microscopy. SPCEs modified with QDs were analysed before and after carrying out the electrodeposition of silver in the same conditions as the voltammetric study but for different times (0, 5, 15, and 30 s). A high fluorescence is observed at the electrode without electrodeposited silver as illustrated in the Figure S4. This fluorescence decreases considerably with increasing electrodeposition times. For 30 s (and superior values), no fluorescence is observed at the electrode surface. This fact means that even at times when the electrochemical saturation is not still occurring (times lower than 120 s as shown in Figure 2), silver is already covering all the surface of the QDs, and the fluorescence is hindered.

This study shows that the selective deposition of silver only at QDs sites can be performed by controlling the deposition parameters. Therefore, localized nanostructures can be generated only where the electrode was modified with quantum dots. Furthermore, depending on the amount of silver and QDs deposited, the size or surface density of the generated nanoparticles can be controlled. The structure of the nanoparticles was studied by performing HRTEM images of a carbon-coated grid in order to carry out the electrodeposition of silver on the grid using very soft conditions to avoid saturation (2 µL of 10 nM QDs solution, 50 µM of silver concentration, 0 V for the electrodeposition potential and 1 s for the electrodeposition time). Figure 3a shows the HRTEM image of unmodified QDs with a monocrystalline and quasi-spherical structure and a size between 10-15 nm. After the electrodeposition, more heterogeneous structures are observed, but, typically, incorporating two clear phases as shown in the Figure 3b (and Figure S5). A phase with a similar structure to the previous image (bare QDs) is observed, but a new darker polycrystalline phase, attributed to silver, appears in the side regions of the QDs forming a Janus-like nanoparticle. EDX analysis (Figure S6) confirmed the visual identification, showing that silver is preferably electrodeposited on the side of the QDs at these electrodeposition conditions.

A possible scheme of the selective deposition over time is shown in Figure 4. At lower times, the reduced silver is deposited on the quantum dots surface in a Janus-like configuration until that the amount of silver saturates the entire surface of the QDs. Considering the quantum dots size (10-15 nm) and the silver nanoparticles size shown in the SEM images after the selective deposition in a SPCE (up to 100 nm, depending on the conditions), the catalytic effect of the QDs is shown even with a multilayer silver structure. After the saturation, two situations could happen: the reduced silver is deposited on the surface of the carbon or over the silver coating the quantum dots. Two kinds of silver particles are noticed in the SEM images when the electrodeposition is carried out after saturation, indicating that the former situation happens. If the latter situation also occurred (as it is likely), no significant thermodynamic/kinetic differences between the two situations are observed in the electrochemical measurements. When the

deposition of silver is carried out with extreme conditions (longer deposition times and/or higher deposition potentials), the silver stripping process at +0.45 V appears to decrease in some cases in an irreproducible way. This fact suggests that the silver deposition over the silver coating the QDs also occurs, and the adsorption effect of silver on QDs is hindered.

The selectivity of the electrodeposition on quantum dots towards other metals soluble in 1M NH_3 such as Co(II), Ni(II) and Cu(II) was evaluated. In the Figure S7, the cyclic voltammograms obtained for solutions of 250 µM of these metals in 1 M NH_3 at bare and QDs-modified screen-printed electrodes are shown. CVs of Co(II) and Ni(II) showed the same processes in bare and QDs-modified electrodes. This fact indicates that the presence of QDs in the electrode surface does not affect the electron transfer from the electrode to the metal ion and no particular interaction metal-QDs is electrochemically visible. For Cu(II), several processes are observed as Cu(I) can be formed in a NH_3 medium. Interestingly, the oxidation process at a more positive potential, which is attributed to the oxidation of Cu(I) to Cu(II) is greatly enhanced in the presence of QDs. Probably, the Cu(I) species generated in the oxidation wave can be stabilized by the QDs and do not suffer disproportionation like it seems at bare electrodes. However, this process does not seem to be due to the selective electrodeposition of Cu on QDs (although, it is a very interesting process to study in depth). Therefore, according to the mechanism proposed here (QDs trap electrons and transfer them to the Ag^+ ions locally surrounding the QDs), the high selectivity towards silver is possibly given by the energy of the electrons that the QDs are capable to donate to the metal (Ag reduction occurs at a lower energy than for these metals). However, the confirmation of this mechanism needs further theoretical/fundamental studies and it is not the scope of the work reported here.

Nucleation of silver nanoparticles on quantum dots

The nucleation of silver particles on quantum dots-modified and bare screen-printed electrodes was carried out. Functionalized surfaces, fabricated using bare and QDs-modified electrodes and the same experimental conditions (-0.2V, 60 s, 250 µM), were studied by scanning electron microscopy, and the micrographs are shown in the Figure 5. For bare carbon electrodes, flower-shaped silver microstructures with a variable size between 1-2 µm are obtained. For QDs-modified electrodes, spherical-shaped silver nanoparticles with homogeneous size around 200 nm are obtained. The data obtained by SEM shows visual evidence that two different ways of particle nucleation and growth occurs at the bare and modified electrodes. The different nucleation and growth of the silver particles was studied after the analysis of the current transient by fitting the experimental data to the theoretical model developed by Scharifker and Hills[31] (see S.I.). This model has been extensively used to analyse the nucleation and growth of electrodeposited metals[32]. As seen in the Figure 6, the experimental data obtained for the silver electrodeposition at different potentials (-0.2, -0.4, -0.5, -0.6 V) on the carbon electrodes followed fairly well the theoretical model for an instantaneous nucleation, indicating a slow growth of nuclei on a small number of active sites. However, on the QDs-modified electrodes, the experimental data followed the theoretical model for a progressive nucleation, which corresponds to a fast growth of nuclei on many active sites. These data agree perfectly with the data obtained in the SEM micrographs, where a larger number of active sites are observed at the QDs-modified electrode.

Localized nanostructures by the selective electrodeposition of silver on quantum dots

As previously mentioned, the selective electrodeposition of silver on quantum dots can be performed by controlling the electrodeposition conditions. Therefore, using a conductive surface partially modified with quantum dots would allow the generation of silver nanostructures only in the area where the QDs were previously added. In order to evaluate structurally the selective electrodeposition, the electrodes were

modified with different patterns of the QDs solution using a low-volume micropipette (0.1-1 µL), and the QDs were left to adsorb for a certain time. The electrodeposition conditions were adjusted to be below the saturation (a deposition potential of -0.1 V with deposition times between 15-60 s and 50-250 µM of silver solution were used) because with inferior solution volumes the saturation of QDs occurs after the deposition of a lower amount of silver. In order to monitor the saturation, linear-sweep voltammograms were performed to control if the bulk stripping process appeared. For specific cases where the deposition conditions were gentle (-0.1 V, 15 s and 50 µM or less), the stripping of silver could be observed using voltammetry but not silver nanoparticles were found in the SEM images. This fact indicates that the nanoparticles generated in this way were really small (< 30 nm) and is very difficult to find them on such rough and opaque surface such as screen-printed carbon. The surface of the modified electrodes was characterized by SEM. Figure 7 shows SEM images (at different magnifications) of a SPCE modified with several drops of 0.5 µL of a 50 nM QDs solution after the electrodeposition of 50 µM of silver for 60 s using -0.1 V. A clear differentiation between the surface modified with QDs and the bare surface is observed. Silver is clearly deposited on the QDs, generating a nanostructured surface only in the modified area, while that on the bare surface no silver is observed. For control purposes, the electrodes were modified only with buffer solution and electrodeposition of silver was performed. Although in some cases, silver was observed on the electrode surface, no preference by the modified areas was found and dispersed silver particles were noticed over the entire surface. Interestingly, as Figure 7b reveals, the silver pattern is observed at a lower magnification because the high quantity of quantum dots and, therefore, of silver nanoparticles generates a visible continuous-like nanostructure. As shown in the Figure 5, with a lower concentration of QDs, the localized nanoparticles can be placed in a more dispersed way instead of a continuous-like nanostructure. The method developed in this work reveals the easy generation of localized nanostructured surfaces by electrodeposition. It can be performed in a short period of time on any conductive surface. If the modification of the electrodes with the QDs solution is carried out using a more

sophisticated automatic instrumentation, a higher resolution, and different types of patterns could be easily generated on the specific surfaces.

Quantum dots detection by the selective electrodeposition of silver

The selective electrodeposition of silver on the quantum dots depends on the amount of quantum dots on the electrode surface. This fact can be used for analytical purposes in electrochemical (bio)sensors, where quantum dots are used as labels. The methodology for biosensing applications could be similar to previously reported works where the biological reaction is carried out in the electrode surface or with the aid of magnetic particles[22,26]. However, instead of quantifying the QDs by metal detection, the electrodeposition of silver should be performed. As a proof-of-concept, the determination of quantum dots was performed using the selective electrodeposition of silver on these nanoparticles and the peak current of the stripping process at the more positive potential was employed as analytical signal. Quantum dots are being widely employed in different applications as biosensing, solar cells, in vivo imaging, and, even in television manufacturing, having an increasing industrial importance[33–35]. The electrochemical detection of QDs have shown a better sensitivity than other established methods employed during the synthesis for quality control of the nanoparticles. Therefore, the electrochemical method could complement these techniques. On the other hand, some of the most used quantum dots are fabricated with heavy metals, and can be potentially toxic[36,37], so its detection in environmental samples could have a wide importance in the coming years if their use continues to grow. Moreover, with the comparison of the method developed in this work with other electrochemical methods previously published, quantitative information about the improved analytical characteristics can be obtained. The experimental procedure was, briefly, as follows: the quantum dots were deposited on the electrode surface until adsorption, and then a solution of 250 µM of silver in 1 M NH_3 was added. The deposition was carried out by applying a potential of -0.2 V for 60 s, and the analytical signal was obtained using differential-pulse voltammetry. As can be observed in the Figure 8,

the voltammetric response was proportional to the particle concentration of quantum dots in the initial solution. The analytical figures of merit obtained (see Table S2) for the determination of quantum dots using this method significantly improves the detection limit obtained by previous works[21,38]. We recently developed a methodology for the determination of quantum dots using screen-printed electrodes by means of an acid attack and subsequent detection of the released cadmium. However, the methodology developed in the present work improves the detection limit by one order of magnitude, decreasing it up to pM. In addition, no acid attack is necessary to release the electroactive metal, thus, simplifying the entire procedure and reducing the analysis time.

This method also has advantages compared to the silver enhancement methodology on gold nanoparticles, previously reported[14,15]. In that case, the silver concentration and the deposition potential and time are extremely important parameters, which must be set very accurately to produce the deposition selectively onto the gold nanoparticles. With the method developed in our work, the analytical signal is a selective stripping process of the silver deposited only on the quantum dots. This process is quite independent of the deposition of silver on the rest of the surface, so that in this case, it is not strictly necessary to fine-tuning the deposition parameters. In order to obtain the highest sensitivity possible, saturating conditions (quantum dots surface should be saturated with silver) should be used, while that the selectivity will be given, as mentioned, by the selective stripping process. This fact means that, although part of the silver is non-selectively deposited, the peak current of the stripping process at the more positive potential will remain proportional to the amount of quantum dots on the surface.

CONCLUSIONS

In this work, the selective electrocatalytic deposition of silver onto the surface of quantum dots is reported. The electrochemical behaviour of the silver deposited on the quantum dots is very different to that of silver

deposited on carbon or on gold nanoparticles, as previously reported. Electrochemical data showed two main things: on the one hand, the silver is strongly adsorbed on the quantum dots showing a selective stripping process at a potential more positive than the stripping process of silver on carbon. On the other hand, the ability to control the deposition selectively allows the generation of surfaces with silver only where quantum dots are previously deposited. This fact can be exploited for the fabrication of localized nanostructured surfaces, which may have direct applicability in the production of functional surfaces or as sensor transducers. A proof of concept is reported for the detection of quantum dots using this method, resulting in a significant improvement of the sensitivity using electrochemical techniques. Therefore, the selective electrodeposition of silver on quantum dots is also a promising method for detection in electrochemical biosensors with quantum dots as labels.

ASSOCIATED CONTENT

SUPPORTING INFORMATION

Briefly, it consists of: fabrication of the Ag/AgCl reference electrode, linear-sweep voltammetry experiments, confocal microscopy imaging, HRTEM imaging and EDX analysis of Ag-QDs nanoparticles, a selectivity study towards other metals, Scharifker-Hills theoretical model and QDs detection procedure. This material is available free of charge via the Internet at http://pubs.acs.org.

AUTHOR INFORMATION

ACKNOWLEDGEMENTS

This work has been supported by the FC-15-GRUPIN-021 project from the Asturias Regional Government and the CTQ2014-58826-R project from the Spanish Ministry of Economy and Competitiveness (MEC). Daniel Martín-Yerga thanks the MEC for the award of a FPI grant (BES-2012-054408).

NOTES

The authors declare no competing financial interest.

FIGURES

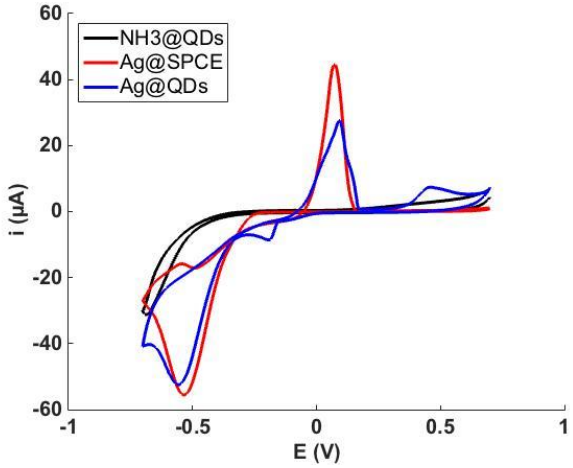

Figure 1. Cyclic voltammetry of silver at a QDs-modified SPCE (blue line), at a bare SPCE (red line) and cyclic voltammetry of NH_3 at a QDs-modified SPCE (black line).

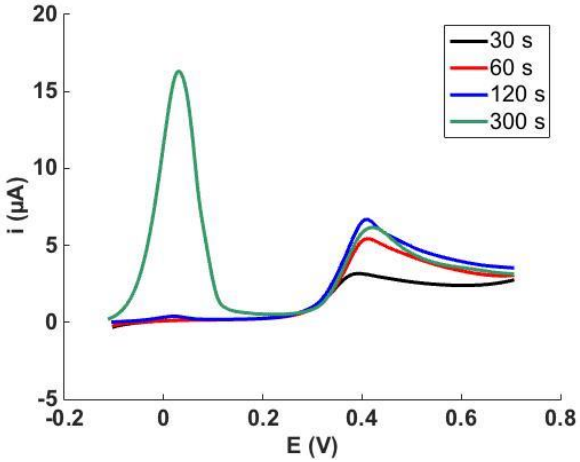

Figure 2. Linear sweep voltammetry from -0.1 to +0.7V of 50 μM of silver after electrodeposition by applying -0.1 V for different times (30, 60, 120, 300 s) at a QDs-modified electrode.

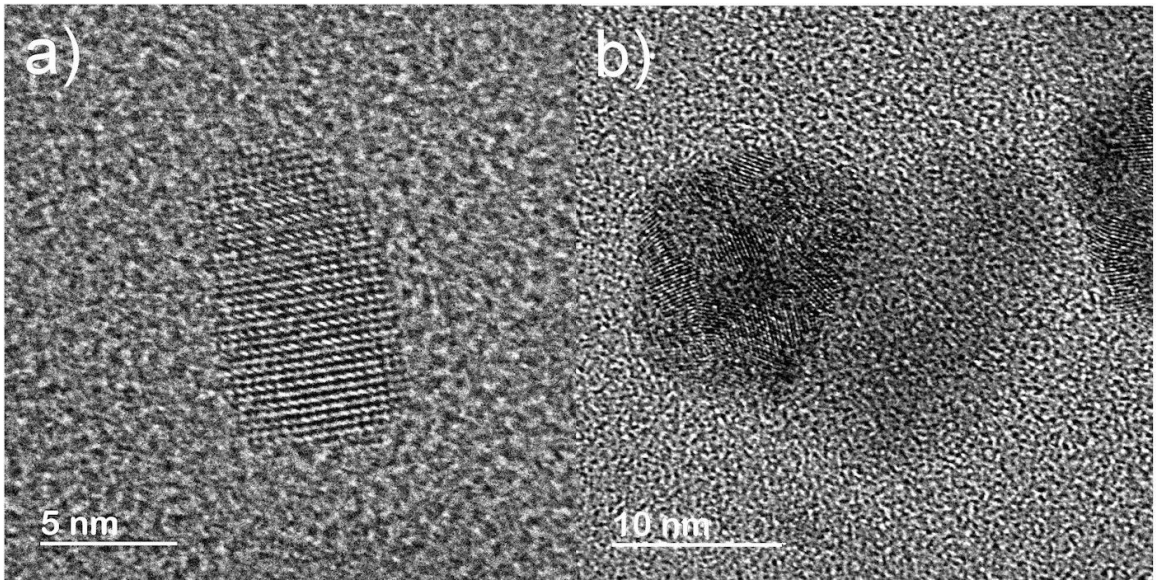

Figure 3. HRTEM image of a carbon-coated grid modified with QDs **(a)**, and modified with QDs after the electrodeposition with silver **(b)**.

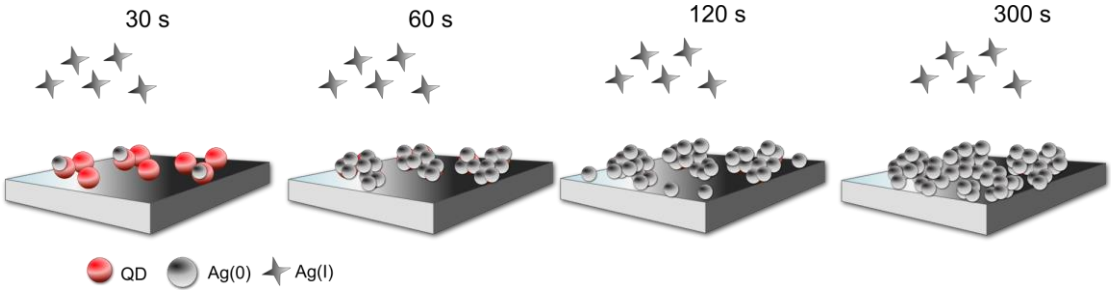

Figure 4. Scheme of the silver electrodeposition on a QDs-modified electrode at different deposition times.

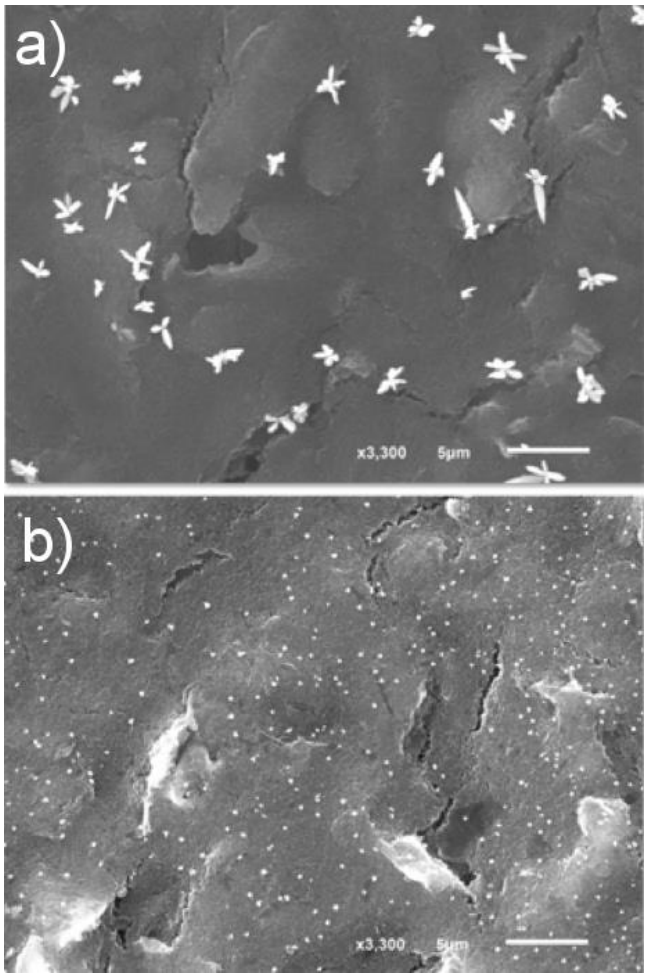

Figure 5. SEM images of **a)** bare SPCE and **b)** QDs-modified SPCE after electrodeposition with silver under the same experimental conditions.

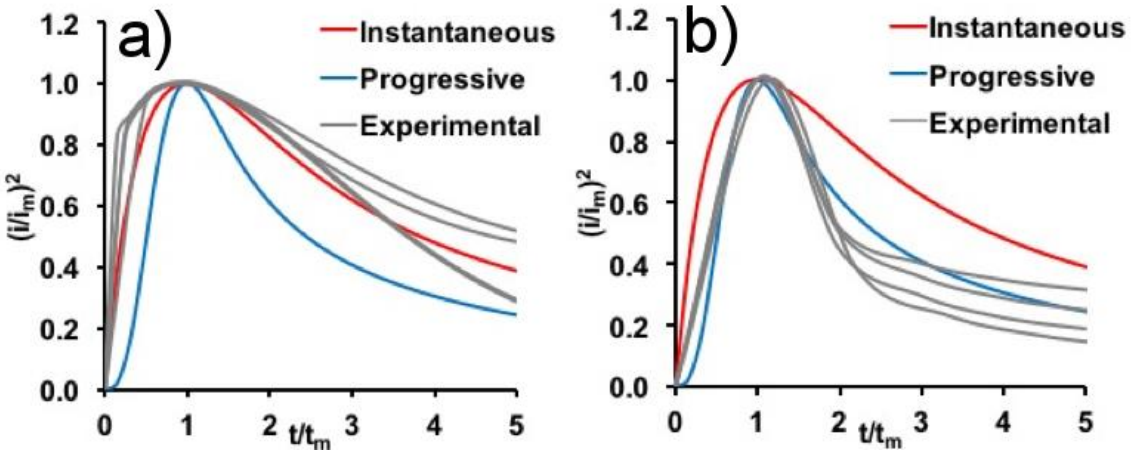

Figure 6. Scharifker-Hills model i-t transients for the electrodeposition of silver on **a)** bare SPCEs and **b)** QDs-modified SPCEs.

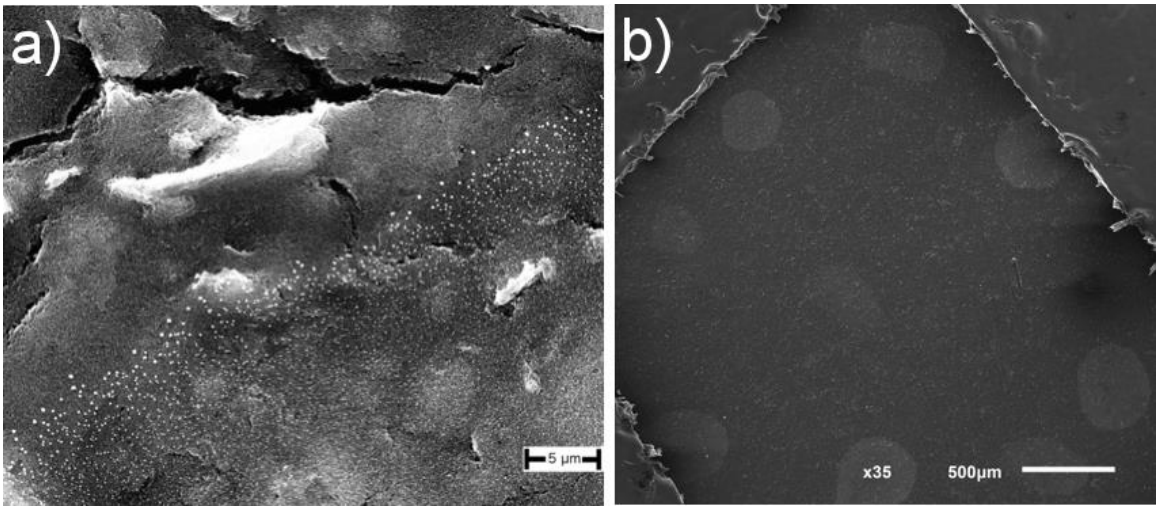

Figure 7. **a)** SEM image of a SPCE, after electrodeposition with silver, partially modified with different drops of a 50 nM QDs solution. In this figure, the edge of a drop is shown to visualize the interface between QDs-modified and bare carbon surfaces. **b)** SEM image of the same electrode at a lower magnification.

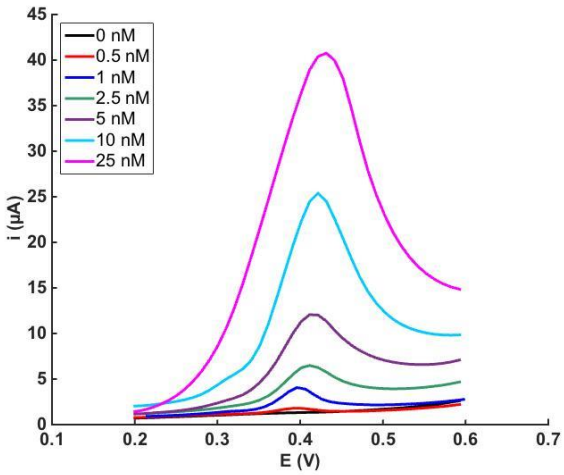

Figure 8. Silver stripping voltammetric responses of SPCEs modified with different QDs concentration.

REFERENCES

(1) Malel, E.; Colleran, J.; Mandler, D. *Electrochim. Acta* **2011**, *56* (20), 6954–6961.

(2) Fedorov, R. G.; Mandler, D. *Phys. Chem. Chem. Phys.* **2013**, *15* (8), 2725–2732.

(3) Liu, L.; Tan, C.; Chai, J.; Wu, S.; Radko, A.; Zhang, H.; Mandler, D. *Small* **2014**, *10* (17), 3555–3559.

(4) Lai, S. C. S.; Lazenby, R. A.; Kirkman, P. M.; Unwin, P. R. *Chem. Sci.* **2015**, *6* (2), 1126–1138.

(5) Fosdick, S. E.; Knust, K. N.; Scida, K.; Crooks, R. M. *Angew. Chemie - Int. Ed.* **2013**, *52* (40), 10438–10456.

(6) Loget, G.; Roche, J.; Gianessi, E.; Bouffier, L.; Kuhn, A. *J. Am. Chem. Soc.* **2012**, *134* (49), 20033–20036.

(7) Loget, G.; Roche, J.; Kuhn, A. *Adv. Mater.* **2012**, *24* (37), 5111–5116.

(8) Quinn, B. M.; Dekker, C.; Lemay, S. G. *J. Am. Chem. Soc.* **2005**, *127* (17), 6146–6147.

(9) Claussen, J. C.; Hengenius, J. B.; Wickner, M. M.; Fisher, T. S.; Umulis, D. M.; Porterfield, D. M. *J. Phys. Chem. C* **2011**, *115* (43), 20896–20904.

(10) Vedala, H.; Sorescu, D. C.; Kotchey, G. P.; Star, A. *Nano Lett.* **2011**, *11* (6), 2342–2347.

(11) Claussen, J. C.; Kumar, A.; Jaroch, D. B.; Khawaja, M. H.; Hibbard, A. B.; Porterfield, D. M.; Fisher, T. S. *Adv. Funct. Mater.* **2012**, *22* (16), 3399–3405.

(12) Miranda-Hernández, M.; Palomar-Pardavé, M.; Batina, N.; González, I. *J. Electroanal. Chem.* **1998**, *443* (1), 81–93.

(13) Hernández-Santos, D.; González-García, M. B.; Costa-García, A. *Electrochim. Acta* **2005**, *50* (9), 1895–1902.

(14) Hernández-Santos, D.; González-García, M. B.; Costa-García, A. *Electrochim. Acta* **2000**, *46* (4), 607–615.

(15) de la Escosura-Muñiz, A.; Maltez-da Costa, M.; Merkoçi, A. *Biosens. Bioelectron.* **2009**, *24* (8), 2475–2482.

(16) Gill, R.; Zayats, M.; Willner, I. *Angew. Chem., Int. Ed.* **2008**, *47* (40), 7602–7625.

(17) Hummon, M. R.; Stollenwerk, A. J.; Narayanamurti, V.; Anikeeva, P. O.; Panzer, M. J.; Wood, V.; Bulović, V. *Phys. Rev. B* **2010**, *81* (11), 115439.

(18) Amelia, M.; Lincheneau, C.; Silvi, S.; Credi, A. *Chem. Soc. Rev.* **2012**, *41* (17), 5728–5743.

(19) Wang, J.; Liu, G.; Rivas, G. *Anal. Chem.* **2003**, *75* (17), 4667–4671.

(20) Wang, J.; Liu, G.; Merkoçi, A. *J. Am. Chem. Soc.* **2003**, *125* (11), 3214–3215.

(21) Martín-Yerga, D.; Bouzas-Ramos, D.; Menéndez-Miranda, M.; Bustos, A. R. M.; Encinar, J. R.; Costa-Fernández, J. M.; Sanz-Medel, A.; Costa-García, A.

Electrochim. Acta **2015**, *166*, 100–106.

(22) Wang, H.; Wang, J.; Timchalk, C.; Lin, Y. *Anal. Chem.* **2008**, *80* (22), 8477–8484.

(23) Kokkinos, C.; Economou, A.; Petrou, P. S.; Kakabakos, S. E. *Anal. Chem.* **2013**, *85* (22), 10686–10691.

(24) Martín-Yerga, D.; González-García, M. B.; Costa-García, A. *Sens. Actuators B* **2013**, *182*, 184–189.

(25) Martín-Yerga, D.; González-García, M. B.; Costa-García, A. *Talanta* **2014**, *130*, 598–602.

(26) Martín-Yerga, D.; Costa-García, A. *Bioelectrochemistry* **2015**, *105*, 88–94.

(27) Ustarroz, J.; Gupta, U.; Hubin, A.; Bals, S.; Terryn, H. *Electrochem. commun.* **2010**, *12* (12), 1706–1709.

(28) Son, D. H.; Hughes, S. M.; Yin, Y.; Paul Alivisatos, A. *Science* **2004**, *306* (5698), 1009–1012.

(29) Huang, K.; Xu, K.; Tang, J.; Yang, L.; Zhou, J.; Hou, X.; Zheng, C. *Anal. Chem.* **2015**, *87* (13), 6584–6591.

(30) Haram, S. K.; Quinn, B. M.; Bard, A. J. *J. Am. Chem. Soc.* **2001**, *123* (36), 8860–8861.

(31) Scharifker, B.; Hills, G. *Electrochim. Acta* **1983**, *28* (7), 879–889.

(32) Day, T. M.; Unwin, P. R.; Macpherson, J. V. *Nano Lett.* **2007**, *7* (1), 51–57.

(33) Yu, W. W.; Chang, E.; Drezek, R.; Colvin, V. L. *Biochem. Biophys. Res. Commun.* **2006**, *348* (3), 781–786.

(34) Nozik, A. J.; Beard, M. C.; Luther, J. M.; Law, M.; Ellingson, R. J.; Johnson, J. C. *Chem. Rev.* **2010**, *110* (11), 6873–6890.

(35) Shirasaki, Y.; Supran, G. J.; Bawendi, M. G.; Bulović, V. *Nat. Photonics* **2013**, *7* (12), 933–933.

(36) Hardman, R. *Environ. Health Perspect.* **2006**, *114* (2), 165–172.

(37) Hoshino, A.; Fujioka, K.; Oku, T.; Suga, M.; Sasaki, Y. F.; Ohta, T.; Yasuhara, M.; Suzuki, K.; Yamamoto, K. *Nano Lett.* **2004**, *4* (11), 2163–2169.

(38) Merkoçi, A.; Marcolino-Junior, L. H.; Marín, S.; Fatibello-Filho, O.; Alegret, S. *Nanotechnology* **2007**, *18* (3), 035502.

SUPPORTING INFORMATION

Electrochemical study and applications of the selective electrodeposition of silver on quantum dots

Daniel Martín-Yerga*, Estefanía Costa Rama and Agustín Costa-García

Department of Physical and Analytical Chemistry, University of Oviedo, Julián Clavería 8, 33006, Oviedo (Spain)

*Email: martindaniel@uniovi.es

Contents

S1. FABRICATION OF THE Ag/AgCl REFERENCE ELECTRODE

The lab-made Ag/AgCl reference electrode was fabricated using a 10-100 µL micropipette tip as holder. The Ag wire (1mm, Alfa Aesar) is covered with AgCl by the application of +0.8 V for 10 min in a solution of 1 M KCl (using another Ag wire as cathode). The salt bridge is generated following a modified procedure found in the literature[1] consisting of an agarose gel with KNO_3. 0.35 g of agarose is added to 25 mL of 0.5 M KNO_3 solution and the mixture is heated and stirred to dissolve the agarose. The micropipette tip is placed in the solution (in a micro test tube), which is allowed to cool overnight to generate the agarose gel. Then, the tip is filled with saturated KCl and the Ag/AgCl wire is placed in the solution. The reference electrode was connected to the potentiostat using alligator clips. The reference electrode was stored in a saturated KCl solution avoiding the light. The good reproducibility in the peak potentials of the voltammograms during the experiments (in different days) showed the good behaviour and stability of the fabricated reference electrode.

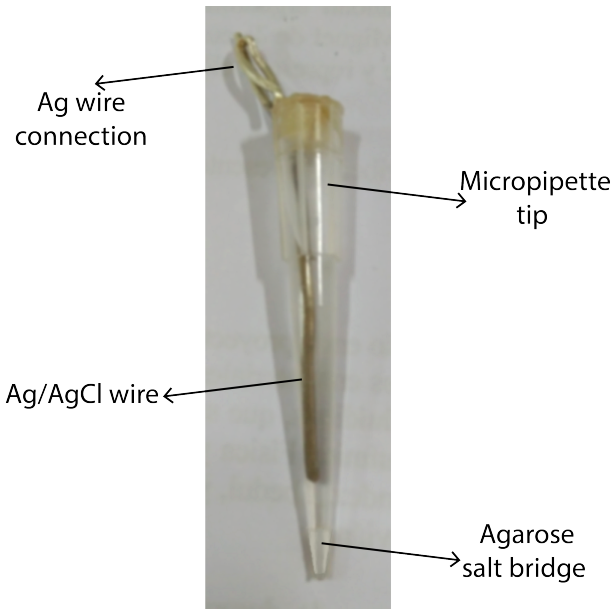

Figure S1. Lab-made Ag/AgCl reference electrode in a micropipette tip.

S2. LINEAR-SWEEP VOLTAMMETRY EXPERIMENTS

Firstly, the linear-sweep voltammetry (LSV) of the reduction/deposition was performed (Figure S2A). As shown in the figure, for an electrode without QDs, a single reduction process occurs at a potential about -0.5 V. This is the usual silver electrodeposition process on carbon surfaces. For a modified electrode, a new reduction process appears at a potential of -0.05 V. This process does not appear for bare carbon electrodes, or when the electrode was modified with QDs but the LSV was only performed with background electrolyte (1 M NH_3). Therefore, this process involves silver and quantum dots, and it behaves very similar to the underpotential deposition of a metal on a metallic surface [2,3]. The reduction of silver in solution is enhanced by the presence of quantum dots in the electrode surface. QDs work as a catalyst for the silver reduction.

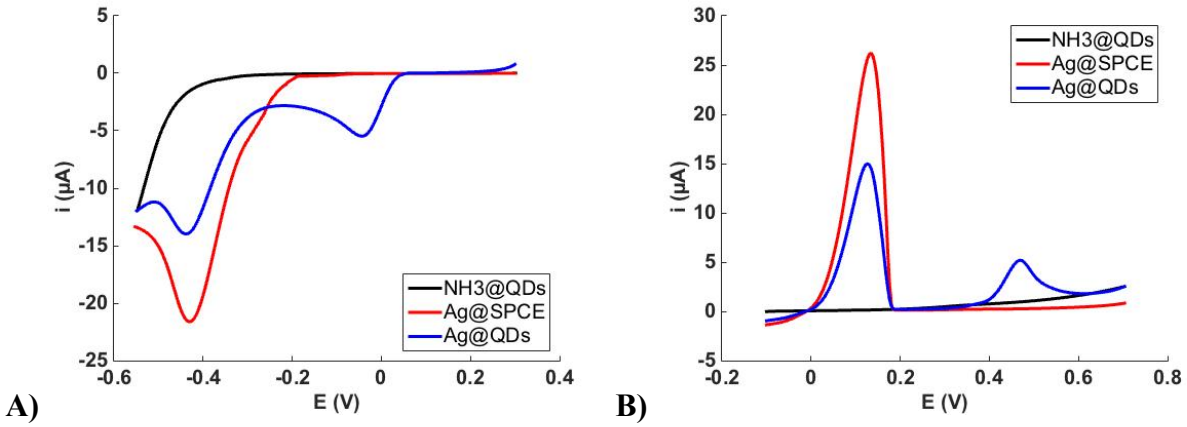

Figure S2. A) Linear sweep voltammetry from +0.3 to -0.55 V for NH_3 at a QDs-modified SPCE (black line), 250 µM of silver at a SPCE (red line) and 250 µM of silver at a QDs-modified SPCE (blue line). **B)** Linear sweep voltammetry from -0.1 to +0.7 V for NH_3 at a QDs-modified SPCE (black line), 250 µM of silver at a SPCE (red line) and 250 µM of silver at a QDs-modified SPCE (blue line) after electrodepositon applying -0.2 V for 60 s.

On the other hand, a LSV study of the stripping processes after the electrodeposition by applying a potential of -0.2 V for 60s was carried out (Figure S2B). In the same way as for the reduction processes, significant differences were found. As shown in the figure, for a bare screen-printed carbon electrode, the typical stripping process of silver on carbon at about +0.05 V appeared. However, when QDs-modified electrodes are used, a new process at a more positive potential (+0.45 V) appeared. This process indicates a strong interaction of silver with the quantum dots, resulting in a more difficult stripping (higher energy stripping). This is significantly different from similar cases such as the electrodeposition of silver or copper on gold nanoparticles, as previously reported [4–6]. In such cases, only one stripping process appears, suggesting that the interaction of the deposited silver with quantum dots is much stronger than in gold nanoparticles.

Limiting-control study

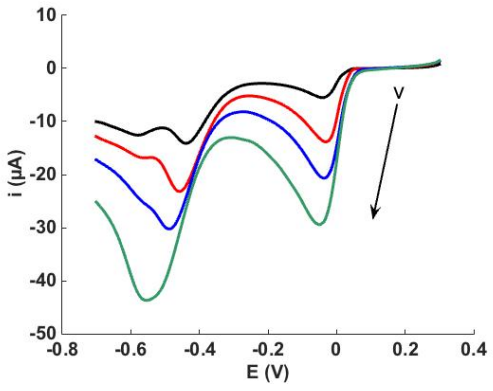

A)

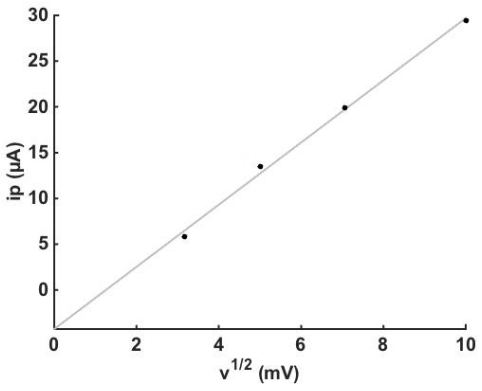

B)

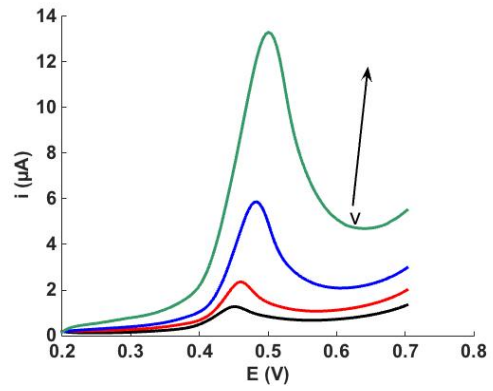

C)

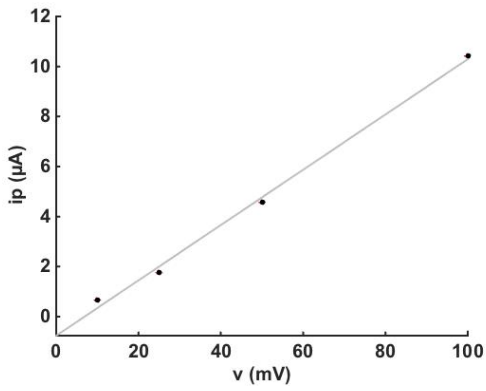

D)

Figure S3. A) Linear sweep voltammetry from +0.25 to -0.7 V of 250 µM silver at different scan rates (10, 25, 50, 100 mV/s) for a QDs-modified electrode. **B)** Relationship between the peak current of the peak at -0.05 V and the square root of the scan rate. **C)** Linear sweep voltammetry from +0.2 to +0.7 V of 50 µM silver at different scan rates (10, 25, 50, 100 mV/s) for a QDs-modified electrode after electrodeposition applying -0.1 V for 60 s. **D)** Relationship between the peak current of the peak at +0.45 V and the scan rate.

S3. CONFOCAL MICROSCOPY ANALYSIS OF THE ELECTRODEPOSITION OF SILVER ON QDs

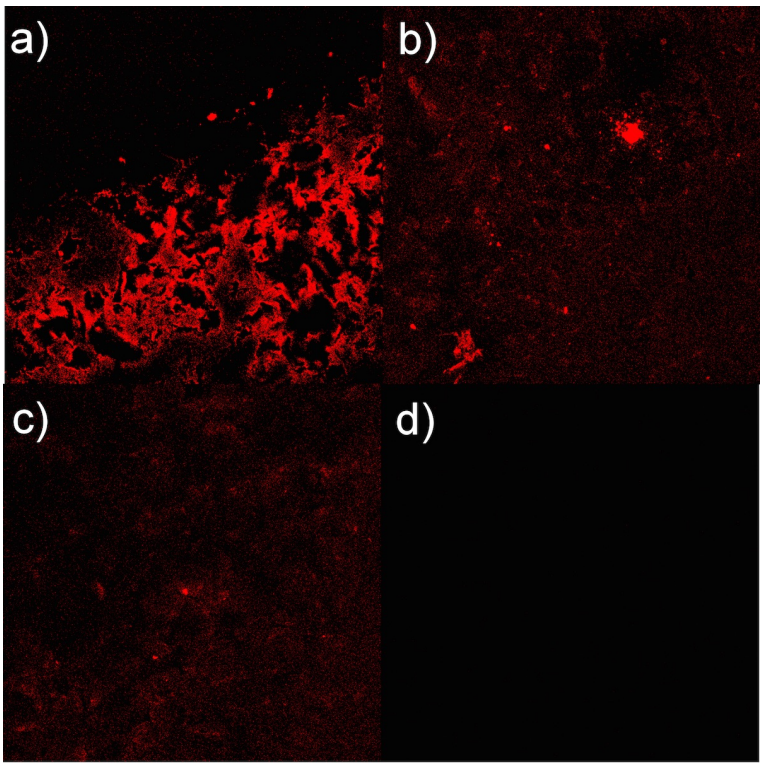

Figure S4. Confocal microscopy of a QDs-modified SPCE without silver electrodeposition (a) and after electrodeposition for 5 (b), 15 (c) and 30 s (d).

S4. HRTEM AND EDX ANALYSIS OF JANUS-LIKE Ag-QDs NANOPARTICLES

HRTEM imaging was performed on a carbon-coated TEM grid. This grid was modified with 2 μL of a 10 nM solution of QDs until dryness. The electrodeposition was carried out in the grid in situ using a solution of 50 μM of Ag (in 1 M NH_3) applying 0 V for 1 s. A grid modified with QDs (without electrodeposited Ag) was used for comparison. Metal electrodeposition on TEM grids have already been reported previously[7] and a similar system was used in our work. Briefly, the TEM grid was placed on a highly ordered pyrolytic graphite (HOPG; NT-MDT, ZYB quality) substrate with the carbon-coated side on top, The HOPG substrate was in contact with a gold-covered metallic sheet connected to the potentiostat. 5 μL of the Ag solution was placed on the TEM grid, only making contact with the carbon membrane, which acts as a working electrode. A platinum wire, acting as auxiliary electrode, was coupled to the Ag/AgCl reference electrode, previously described in section S1.

Quite different HRTEM images were obtained for the QDs-modified grid after the electrodeposition of silver. As mentioned in the main manuscript, a darker phase, attributed to polycrystalline silver, appears coating the QDs, as shown in Figure 3 of the main manuscript and in the Figure S5 (at a lower zoom resolution). In most of the nanoparticles, silver is preferentially localized on one side of the QDs, although in some cases silver is coating almost completely the QDs. This fact indicates that silver begin to grow preferentially in some location of the QD and then keep growing over all the nanoparticle.

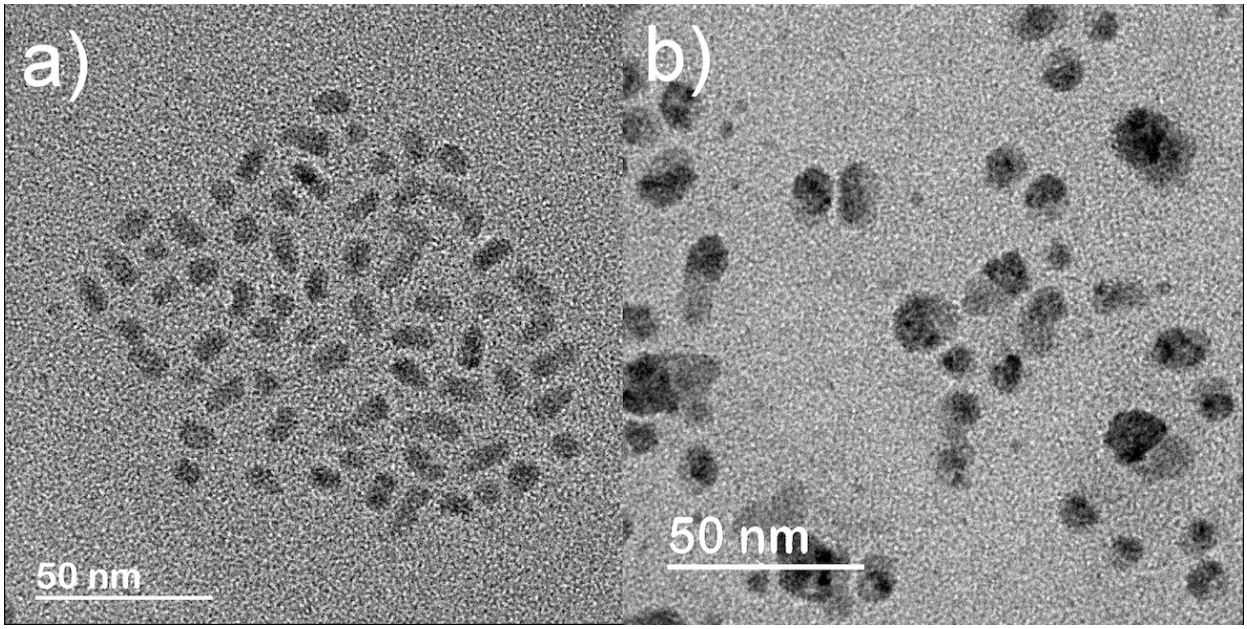

Figure S5. HRTEM images of the QDs nanoparticles (a) and Ag-QD Janus-like nanoparticles generated by the selective electrodeposition method (b).

Energy-dispersive X-ray spectroscopy (EDX) was carried out in the Scanning Transmission Electron Microscopy (STEM) mode in order to confirm the material of the different phases displayed in the obtained images. Although the STEM did not allow a resolution as high as HRTEM, a clear difference in the composition of the different phases was found, confirming that the darker phase was composed mainly of Ag coating the QDs (as the composition also showed S and Se in these areas). S and Se were used as elements to confirm the presence of QDs due to the interference between the Cd and Ag and Zn with Cu (main material of the grid). Figure S6 shows an EDX profile of the Janus-like particles. It can be seen as the Ag is preferably located in a side area of the QDs, whereas in the opposite area, although Ag is also detected, the contribution to the total composition is lower.

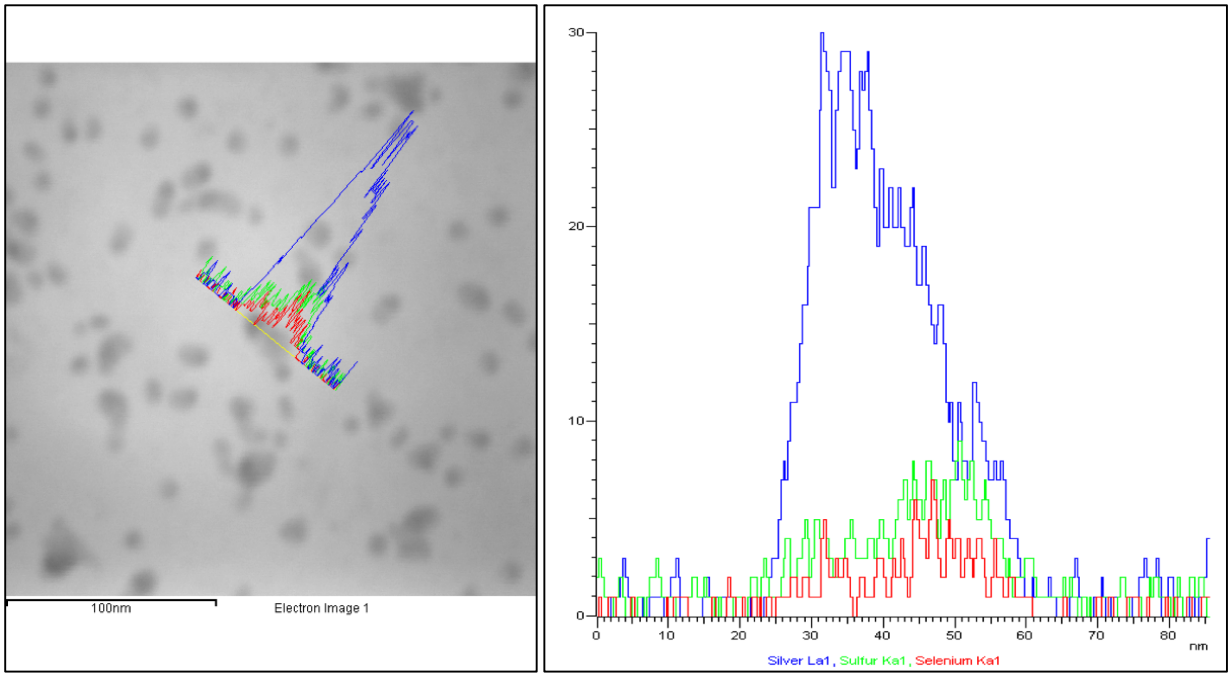

Figure S6. STEM image and composition profile (in atomic percentage) of the observed Janus-like Ag-QD nanoparticles. Profile lines show the composition of silver (blue), sulfur (green) and selenium (red).

S5. SELECTIVITY STUDY TOWARDS THE ELECTRODEPOSITION OF OTHER METALS

Cyclic voltammograms of Co(II), Ni(II) and Cu(II) at bare and QDs-modified screen-printed electrodes are shown in the Figure S7. Zn(II) was also tested but it did not show any process from -1.3 V to +0.8 V (data not shown). For Co(II), two cathodic processes are observed, the first wide peak attributed to the reduction of O_2 (as stated in blank measurements (data not shown)), and a sharper peak at -1.1 V attributed to the reduction of Co(II) to Co(0). Two anodic peaks are observed in the reverse wave, attributed to the oxidation of Co(0) to Co(II) and Co(II) to Co(III), respectively. For Ni(II), two cathodic processes are also observed, attributed to the reduction of O_2 and a very small peak close to the hydrogen evolution attributed to the reduction of Ni(II) to Ni(0). In this case, one anodic peak is observed, attributed to Ni(0) to Ni(II) oxidation. It seems

like some process is observed very close to the evolution of oxygen (as can be seen by the current increment), which could be attributed to the oxidation of Ni(II) to Ni(III), but it is not very well resolved to confirm it. However, no difference between the bare and QDs-modified electrodes was noticed for Co and Ni.

Cu(II) voltammetry is an interesting case. Although, the same number of processes are observed at both electrodes, there are some differences in the potentials and peak currents. The cathodic processes can be attributed to the following reductions: Cu(II) to Cu(I) and Cu(I) to Cu(0) (probably coupled with oxygen reduction). At bare SPCEs, Cu(II) to Cu(I) is a quite wide process as it could be coupled to the oxygen reduction, and a small process attributed to Cu(I) to Cu(0) reduction can also be observed. At QDs-modified electrodes, the Cu(II) to Cu(I) reduction peak is sharper but with a lower peak current in comparison to bare electrodes, while the Cu(I) to Cu(0) process appears also sharper and higher in current. The first anodic process (Cu(0) to Cu(I)) seems quite similar in both electrodes except in the peak potential, which it has shifted to positive potentials at the SPCE electrode. However, the greater difference is noticed in the Cu(I) to Cu(II) oxidation. At bare electrodes, a very small process, almost totally inhibited, is observed at -0.05V. This fact indicates that in this timescale very amount of Cu(I) is stable in the solution and is available for the oxidation. It has probably suffered disproportionation to Cu(II) and Cu(0), something similar can be seen in the cathodic wave (as the Cu(I) to Cu(0) is quite small). At QDs-modified electrodes a peak current 20 times higher is observed for the Cu(I) to Cu(II) oxidation. It seems that QDs are able to stabilize the Cu(I) ions, which then can be oxidized to Cu(II).

However, even with the interesting behaviour of Cu(II) at QDs electrodes, it does not show a selective electrodeposition (catalytic reduction) or selective stripping (adsorption) in comparison to the bare electrode as have been displayed by silver.

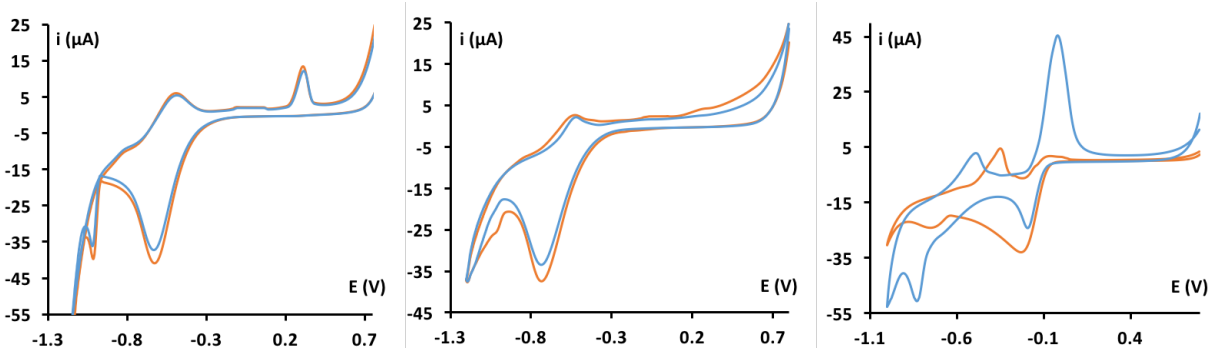

Figure S7. Cyclic voltammograms for Co(II), Ni(II) and Cu(II) on a bare screen-printed carbon electrode (orange line) and a QDs-modified screen-printed electrode (blue line).

S6. SCHARIFKER-HILL MODEL FOR NUCLEATION STUDIES

The nucleation and growth of the silver particles at bare screen-printed electrodes and modified with QDs was studied by analysing the current-time (i-t) transients in a chronoamperometric experiment. I-t transients were recorded in which the electrode potential was stepped from open circuit to different potentials -0.2, -0.4, -0.5 and -0.6 V. Electrode surface was previously modified with 10 µL of a 10 nM QDs solution.

I-t transients of the electrodeposition process were analysed following the Scharifker-Hills theoretical model [8]. In this model, there are two limiting nucleation mechanisms: instantaneous and progressive. The instantaneous nucleation corresponds to a slow growth of nuclei in a small number of active sites. The progressive nucleation corresponds to a fast growth of nuclei in many active sites.

The instantaneous nucleation in this model is described by the following equation:

$$\left(\frac{i}{i_m}\right)^2 = 1.9542\left(\frac{t}{t_m}\right)^{-1}\left\{1 - exp\left[-1.2564\left(\frac{t}{t_m}\right)\right]\right\}^2 \quad \textbf{(S1)}$$

where i is the current density, i_m is the maximum current density, t is time and t_m is the time at the maximum current.

The progressive nucleation can be expressed by the following equation:

$$\left(\frac{i}{i_m}\right)^2 = 1.2254\left(\frac{t}{t_m}\right)^{-1}\left\{1 - exp\left[-2.3367\left(\frac{t}{t_m}\right)\right]\right\}^2 \quad \textbf{(S2)}$$

The experimental i-t transients were analysed with these expressions using the experimental obtained values for imax and tmax.

An expression to estimate the nuclei population density was also predicted for this model:

$$N_0 = 0.065\left(\frac{1}{8\pi C_0 V_m}\right)^{1/2}\left(\frac{nFC_0}{i_m t_m}\right)^{1/2} \quad \textbf{(S2)}$$

where n is the number of electrons involved, F is the Faraday constant, C_0 is the concentration of species in bulk and V_m is the molar volume. Table S1 shows the estimated silver nuclei population densities deposited at -0.2 V for bare SPCEs and QDs-modified electrodes using a 250 μM silver solution. In good agreement with the theoretical model a greater number of active sites are calculated for a progressive nucleation as the produced at QDs-modified electrodes.

	-0.2 V SPCE	**-0.2 V QDs**
N_0 (particles/cm^2)	3.8x10^5	8.1x10^8

Table S1. Estimated nuclei population densities deposited at -0.2 V for bare SPCEs and QDs-modified electrodes using a 250 μM silver solution.

As the stripping process is controlled by the adsorption, the following equation can be used with the data from Figure S3 to estimate the amount of adsorbed silver on the QDs:

$$i_p = \frac{n^2F^2A\Gamma^*}{4\,R\,T}v \quad \textbf{(S4)}$$

where i_p is the peak current, n is the number of electrons, F is the Faraday constant, A is the surface area, Γ^* is the surface concentration, v is the scan rate, R is the gas constant and T is the temperature.

As saturation conditions are employed in this case (electrodeposition using -0.2 V for 60 s and 250 μM of silver), the maximum amount of adsorbed silver that can produce the catalytic process

can be estimated. The estimated value under these conditions was $1.3x10^{-17}$ moles/QD. After the deposition of this amount of silver, the behaviour of the silver deposited over QDs will be similar to the silver deposited on the carbon surface.

S7. QUANTUM DOTS DETECTION PROCEDURE

Using different particle concentrations of QDs on the modified electrode, the selective stripping peak current (at +0.45 V) was found proportional to the QDs concentration. Therefore, a procedure for the electrochemical detection of QDs was developed using the selective electrodeposition of silver on these nanoparticles. The methodology is described in the main text. Deposition potential and time were optimized to obtain the highest analytical signal. No signal is observed at the stripping potential for a bare electrode, even using the more extreme deposition potential and time tested, highlighting the high selectivity of this process.

The peak current obtained was linearly proportional to the particle concentration of QDs in the solution following the equation: i (μA) = 1.57 [QDs] (nM) + 0.007, $R^2 = 0.996$. The linear range obtained was from 0.5 to 25 nM, and the limit of detection, calculated as the concentration corresponding to three times the standard deviation of the estimate, was 130 pM. The calibration plot is shown in the Figure S8. With this methodology, the detection limit is significantly improved to previously reported electrochemical detection of quantum dots, even with an acid digestion (Table S2).

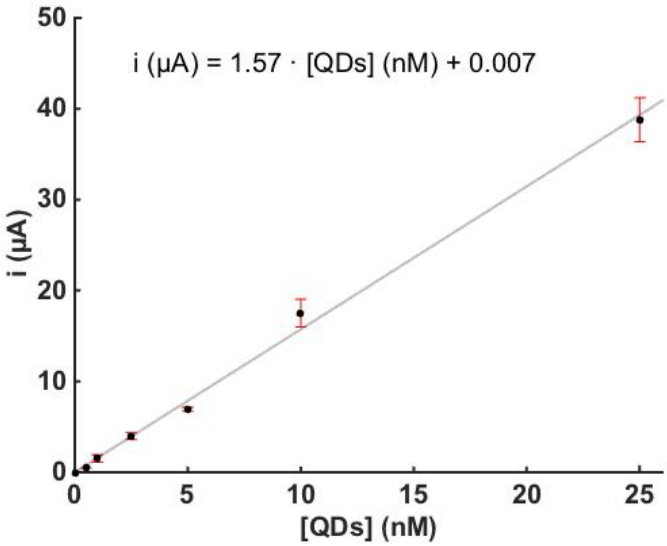

Figure S8. Calibration plot representing the peak current versus the particle concentration of the QDs solution used for the modification of the electrode surface (0, 0.5, 1, 2, 5, 10, 25 nM).

Reference	Linear range	Sensitivity	Limit of detection
[9]	8 – 230 μM	0.05 μA/μM	8 μM
[10]	5 – 200 nM	0.23 μA/nM	2.6 nM
This work	0.5 – 25 nM	1.57 μA/nM	130 pM

Table S2. Analytical figures of merit of several electrochemical methodologies for QDs detection using screen-printed electrodes.

REFERENCES

[1] R. Barlag, F. Nyasulu, R. Starr, A Student-Made Silver–Silver Chloride Reference Electrode for the General Chemistry Laboratory:~ 10 min Preparation, J. Chem. Educ. 91 (2014) 766–768.

[2] E. Herrero, L.J. Buller, H.D. Abruña, Underpotential deposition at single crystal surfaces of Au, Pt, Ag and other materials, Chem. Rev. 101 (2001) 1897–930.

[3] E. Herrero, H.D. Abruña, Underpotential Deposition of Mercury on Au(111): Electrochemical Studies and Comparison with Structural Investigations, Langmuir. 13 (1997) 4446–4453.

[4] D. Hernández-Santos, M.B. González-García, A. Costa-García, Electrochemical determination of gold nanoparticles in colloidal solutions, Electrochim. Acta. 46 (2000) 607–615.

[5] A. de la Escosura-Muñiz, M. Maltez-da Costa, A. Merkoçi, Controlling the electrochemical deposition of silver onto gold nanoparticles: reducing interferences and increasing the sensitivity of magnetoimmuno assays., Biosens. Bioelectron. 24 (2009) 2475–2482.

[6] X. Mao, J. Jiang, Y. Luo, G. Shen, R. Yu, Copper-enhanced gold nanoparticle tags for electrochemical stripping detection of human IgG., Talanta. 73 (2007) 420–4.

[7] J. Ustarroz, U. Gupta, A. Hubin, S. Bals, H. Terryn, Electrodeposition of Ag nanoparticles onto carbon coated TEM grids - A direct approach to study early stages of nucleation, Electrochem. Commun. 12 (2010) 1706–1709.

[8] B. Scharifker, G. Hills, Theoretical and experimental studies of multiple nucleation, Electrochim. Acta. 28 (1983) 879–889.

[9] A. Merkoçi, L.H. Marcolino-Junior, S. Marín, O. Fatibello-Filho, S. Alegret, Detection of cadmium sulphide nanoparticles by using screen-printed electrodes and a handheld device., Nanotechnology. 18 (2007) 035502.

[10] D. Martín-Yerga, D. Bouzas-Ramos, M. Menéndez-Miranda, A.R.M. Bustos, J.R. Encinar, J.M. Costa-Fernández, et al., Voltammetric determination of size and particle concentration of Cd-based quantum dots, Electrochim. Acta. 166 (2015) 100–106.